Robotica (2018) volume 36, pp. 1822–1835. © Cambridge University Press 2018
doi:10.1017/S0263574718000759

Design analysis and optimization of 6-DOF telemanipulator based on performance indices

Seungnam Yu†*, Soonwoong Hwang‡, Jongkwang Lee†, Byungsuk Park† and Hyojik Lee†

† *Korea Atomic Energy Research Institute, Yuseong-gu, Daejeon 34057, Korea*
‡ *Hanyang University, Sangnok-gu, Ansan, Gyeonggi-do 15588, Korea*

(Accepted July 21, 2018. First published online: September 14, 2018)

SUMMARY

In contrast to general industrial robots, which are operated in normal environments and are easily accessible by human workers, telemanipulators are typically designed to perform specific and extreme tasks in hazardous areas. Teleoperation systems are difficult-to-equip fully intuitive or automated control systems because these are the kinds of manipulator systems used as substitutes to perform tasks that humans have to guide directly because they may require tough, sensitive, or sophisticated handling motions. Basically, these kinds of tasks are difficult to remotely perform through a slave manipulator operated by a human unless modification and optimization of the system are conducted. In this regard, the target system dealt within this study has similar disadvantages even though it has a high degree of freedom (DOF) arm structure. The performance of the current system was quantitatively evaluated to optimize the structure according to the considered main tasks. This work presents the various performance indices utilized and analyzes the current design of the considered telemanipulator system. An optimal design approach using the parameters associated with the frequent motions of the considered 6-DOF telemanipulator is then proposed based on the conducted analyses.

KEYWORDS: Telemanipulator, Performance index, Condition number, Manipulability ellipsoid, Modified dynamic conditioning index

1. Introduction

In the case of robot manipulators, certain parameters, such as the joint combinations, degrees of freedom (DOFs), and the length/weight ratio of the linkage, are designed based on the performance requirements and the tasks to which they are dedicated. Therefore, one of the important aspects of manipulator design is to select and analyze the parameters associated with the considered performances.[1,2] In this regard, many studies were conducted, and various proposals were made for the manipulator design parameters using optimization approaches and evaluations performed through simulations. Among the abundant cases, relatively recent studies included those by Singh and Rastegar[3] and Niku.[4]

Each telemanipulator is generally designed for a specified extreme task performed in a hazardous area, which is in contrast to general industrial robots that operate in a normal atmosphere and are easy-to-access by human workers. This kind of telemanipulator system is substituted to perform tasks that humans are hard to handle directly as those may require tough, dangerous handling motions. Moreover, it is not proper to equip intelligent or sophisticated control systems because the telemanipulator system have to be performed properly in a hazardous area by operator's direct command for every step except the special cases of programmable and repetitive motions. Consequently, these kinds of remote handling tasks are difficult to perform through a slave manipulator operated by a human unless the working conditions are modified and optimized for teleoperation. In this regard, the target

* Corresponding author. E-mails: snyu@kaeri.re.kr, hswfile@gmail.com, leejk@kaeri.re.kr, nbspark@kaeri.re.kr, hyojik@kaeri.re.kr

system dealt within this study has similar disadvantages even though it has a high-DOF arm structure. The performance of the current system is quantitatively evaluated herein to optimize the structure according to the considered main tasks.

This paper presents the various performance indices utilized and analyzes the current design of the considered telemanipulator system. Optimal design approaches using the parameters associated with the frequent motions of the considered 6-DOF telemanipulator are proposed based on the conducted analyses. The considered performance criteria are dexterity and energy efficiency. Dexterity refers to the ability to move in arbitrary directions as easily as possible. First, we need to improve dexterity to properly perform the main tasks. To do this, the initial configuration and link length are determined using condition number (CN)[5] and manipulability ellipsoid (ME)[6] and used to confirm the isotropy of the end-effector motion. The modified dynamic conditioning index (MDCI)[7] is then applied as a dynamic performance index to appropriately distribute the elements of the mass–inertia matrix of the manipulator for the enhancement of the energy efficiency because the dynamic performance could be evaluated through kinetic energy. As a final step, a genetic algorithm (GA) is used to acquire optimized results for many parameters included in high-nonlinearity formulations because GA can avoid falling into local optima.[8]

2. Bridge-Transported Dual-Arm Servo-Manipulator (BDSM)

2.1. Basic information

The target system dealt within this study is operated in a specially designed gas-tight cell filled with argon. This facility is called PRIDE (PyRoprocess Integrated inactive DEmonstration facility) and designed for various kinds of pyroprocessing experiments.[9,10] The pyroprocessing process requires an inert atmosphere, and the level of oxygen and moisture must be controlled. Therefore, operators are not allowed to access the inside of the cell, while it is in operation. In this regard, two kinds of telemanipulator systems are installed in PRIDE. The first system is a Mechanical Master–Slave Manipulator (MSM). This MSM is applicable to tasks requiring low payload and high dexterities. Based on operation experience and surveys, operators feel relatively more comfortable while using the MSM than while using the BDSM, which is the other manipulator because the MSM is attached to the wall, and the master's hand side always coincides with that of the slave. The second system is a servo-type manipulator, called BDSM, which travels through the bridge. With this kind of system, it is possible to cover a large area with a higher payload than the MSM. However, unlike with the MSM, the master's hand side does not always coincide with the slave's because the body of the slave is freely rotatable. Moreover, the working window of the argon cell is difficult to utilize to watch the slave because it is generally far from the master device and the operator.

2.2. Kinematic structure

The BDSM has a dual-arm structure, and each arm is designed to handle a maximum weight of 20 kg with 6-DOF in the remote area. To do this, the weight and the inertia of each linkage had to be minimized to reduce the burden on each joint. Fig. 1 shows the configuration and kinematic structure of the BDSM arm.

The entire power transmission was built with a tendon-driven mechanism to concentrate the actuator's weight of each joint to the shoulder part. Each arm was integrated on a rotatable plate module connected with the telescopic mast. The trolley of the telescopic mast can be moved through the bridge and rail.[11,12] Fig. 2 describes the available motions of each joint of the BDSM.

The BDSM arm has a total of 6-DOF for each arm, and is designed to perform universal and versatile motions. Operators manipulate the slave arm using a master device with the same configuration as the slave. Typically, operators can perform the teleoperation work through the camera view attached to the BDSM arm. From a kinematic point of view, the BDSM arm can be stable with a high dexterity motion. Fig. 3(b)–(e) shows that the end-effector can maintain the considered straight-line motion of Fig. 3(a) within the small variations of roll–pitch–yaw angle. Fig. 4 describes the reachable work space of the BDSM.

2.3. Motions of the BDSM in the argon cell facility

The BDSM was originally designed to perform universal operations in PRIDE. However, the main equipment and devices associated with the BDSM allow it to perform several kinds of maintenance

https://doi.org/10.1017/S0263574718000759 Published online by Cambridge University Press

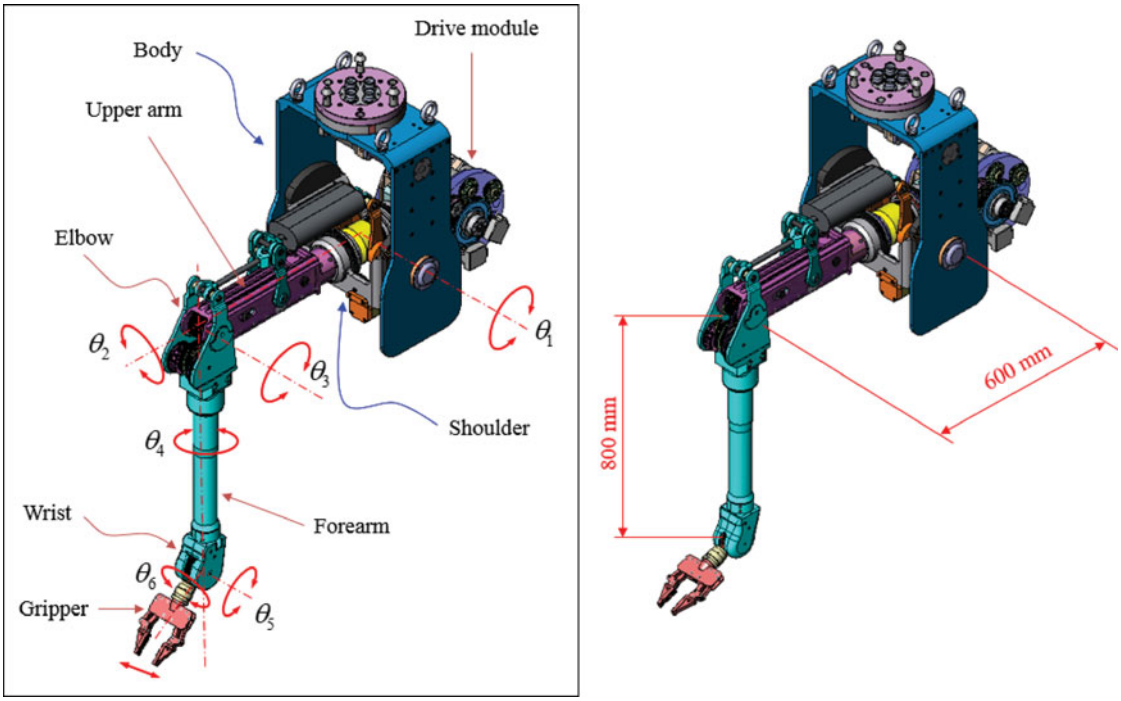

Fig. 1. Configuration of the BDSM arm.

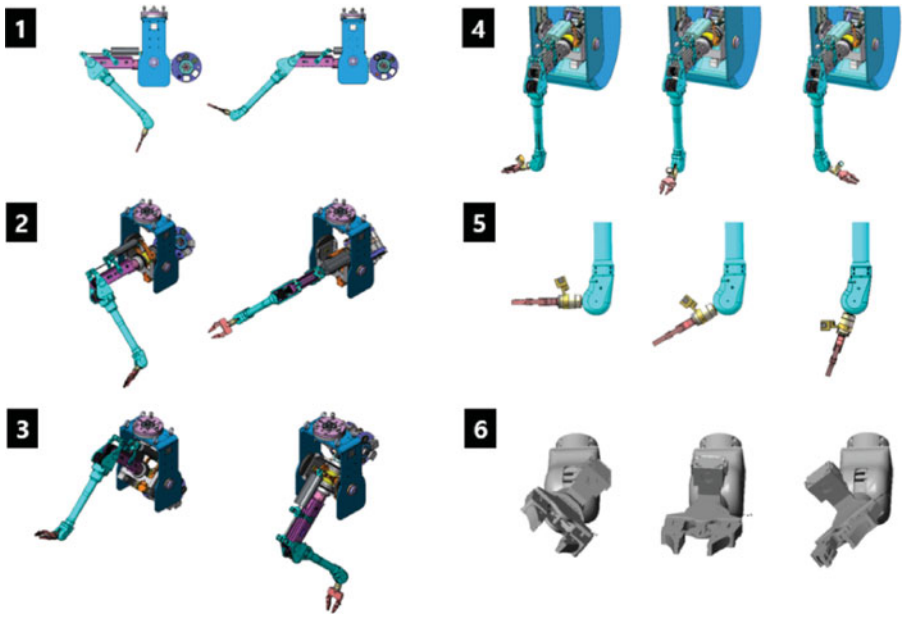

Fig. 2. Available motions of the BDSM arm for each joint: (1) Elbow motion. (2) Shoulder abduction/abduction. (3) Shoulder extension/flexion. (4) Lower arm external/internal rotation. (5) Wrist extension/flexion. (6) Wrist external/internal rotation.

tasks that have become routine. The typical motions of the BDSM are classified subsequently. In addition, among the motions, common motions, such as the vertical and horizontal backward–forward motions, can be identified. The motions shown in Figs. 5 and 6 could be considered easy motions in normal situations. However, as stated earlier, they are relatively difficult to perform in remote areas. That is, the operator is far from the worksite, and operator's visual information is extremely limited because he/she can only use the camera system to view the worksite. Under these conditions,

https://doi.org/10.1017/S0263574718000759 Published online by Cambridge University Press

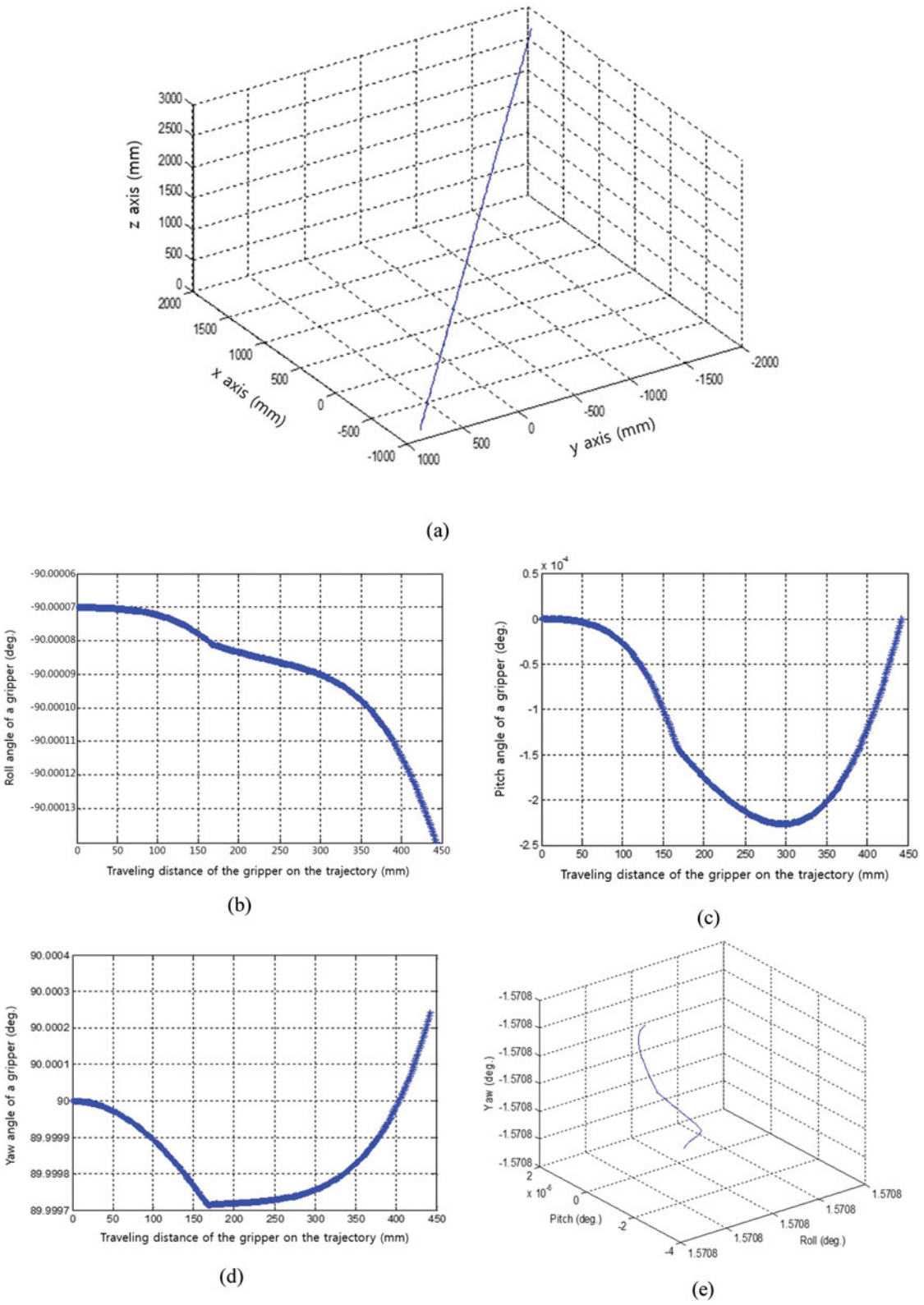

Fig. 3. Stability of the BDSM gripper in the considered straight-line motion while maintaining the gripper's original posture. (a) Considered trajectory of the BDSM arm's end-effector. (b) Variation of roll angle of a gripper of the BDSM. (c) Variation of pitch angle of a gripper of the BDSM. (d) Variation of yaw angle of a gripper of the BDSM. (e) Variations of roll–pitch–yaw angle of the BDSM while moving through the considered trajectory of Fig. 3(a).

https://doi.org/10.1017/S0263574718000759 Published online by Cambridge University Press

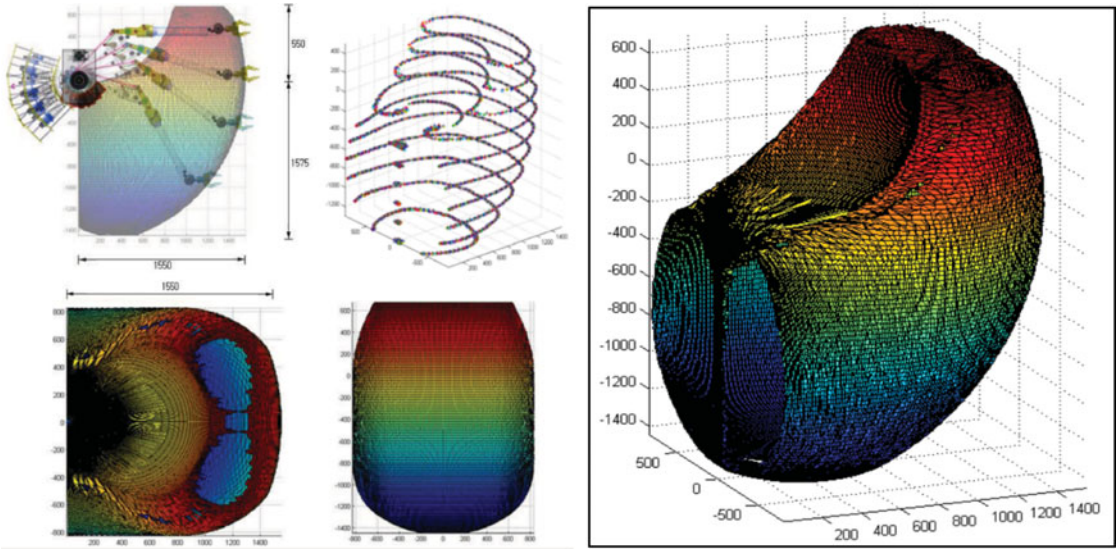

Fig. 4. Analysis of the working space of the originally designed BDSM.

Fig. 5. Considered motions for optimization in this study.

maintaining the correct vertical and horizontal backward–forward motions of the BDSM arm must be accomplished through the operator's sense, experience, and camera vision.

Moreover, the skill and sense of operators can significantly vary, which is not a suitable situation for such a highly sensitive work. Fully satisfying the operator's visual needs is also difficult because visually aligning the working arm and the camera is an extremely difficult process. Furthermore, the lack of alignment could result in the operator having to rely on guesswork, resulting in a relatively low-quality manipulation work. In this regard, the current BDSM arm needs to be analyzed, and improvements must be made to the arm configuration for future versions of the manipulator system to ensure better performance on highly repetitive tasks. To this end, we perform several performance index analyses in the ensuing sections.

3. Application of the Performance Indices

In essence, the major kinematic performances include dexterity because the considered manipulator should be able to perform diverse tasks in the confined cell and dexterity index shows the degree to which the manipulator's end-effector can reach arbitrary positions. In this study, the dexterity index is investigated to improve the performance for the considered motions. It is determined by the link length and configuration of the manipulator arm, and can be measured using the CN and ME based on a Jacobian matrix. CN is utilized to select the initial linkage length and posture, and ME is applied

https://doi.org/10.1017/S0263574718000759 Published online by Cambridge University Press

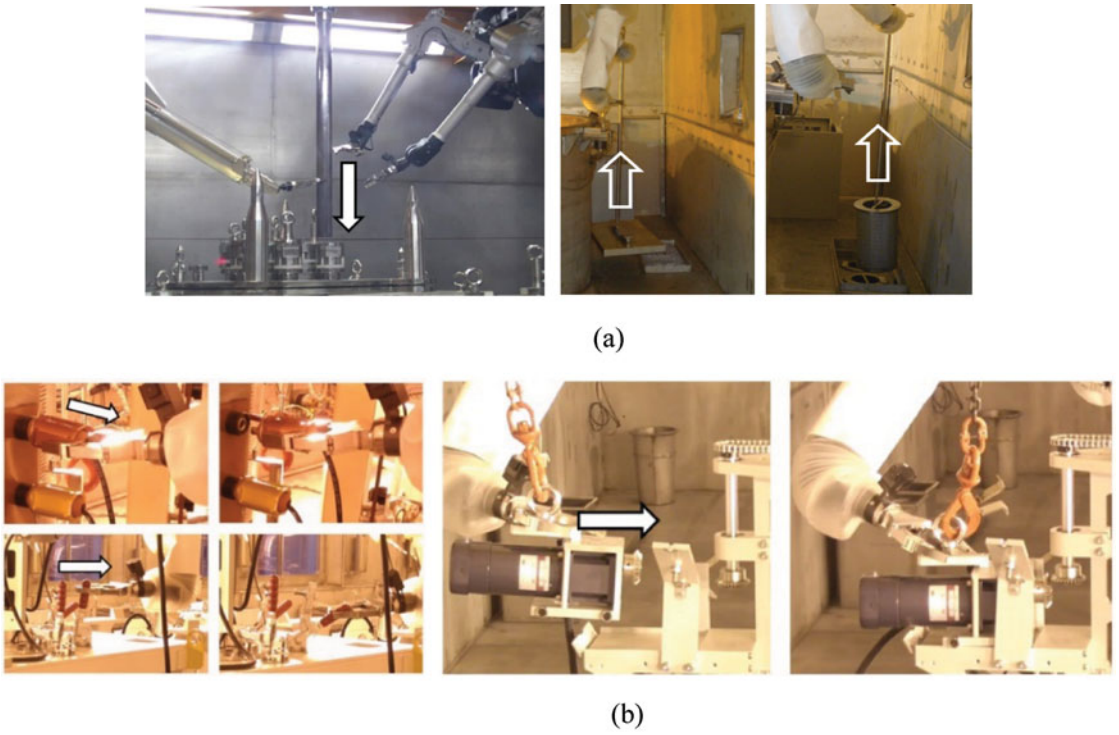

Fig. 6. Examples of the considered motions in PRIDE. (a) Vertical motion by the BDSM arm. (b) Horizontal motion by the BDSM arm.

to visualize the isotropy of the end-effector in the working area. Additionally, in the design process of the manipulator, the lightness of each arm linkage could be an important factor because a lighter linkage requires a smaller actuator for the same payload. The type of actuator and joint connecting each linkage herein is limited to the rotary and revolute types, respectively. These dynamic properties can be analyzed through the mass–inertia matrices obtained from the dynamic models. MDCI was selected to measure the dynamic performance. In this regard, dexterity and energy efficiency are considered as primary criteria for the kinematic and dynamic simulations of this study. Following sections show the detail approaches based on these criteria.

3.1. Condition number (CN)

In designing the BDSM, the end-effector of the arm should move as easily as possible in arbitrary directions because the tasks in the argon cell are diverse. CN is an analytical tool that can quantitatively measure this property. Let $f : N \rightarrow M$ denote the forward kinematic map from the joint space N to the end-effector space M. Eq. (1) is obtained as follows by differentiating f:

$$\dot{\boldsymbol{x}} = \boldsymbol{J}(\boldsymbol{q})\,\dot{\boldsymbol{q}} \tag{1}$$

where $\dot{\boldsymbol{x}} \in \mathbb{R}^{\boldsymbol{m}}$ is the velocity vector of the end-effector; $\boldsymbol{q} \in \mathbb{R}^{\boldsymbol{n}}$ is the displacement vector of the joint; and $\mathbf{J} \in \mathbb{R}^{\boldsymbol{m}\times\boldsymbol{n}}$ is a Jacobian matrix describing the relationship between joint velocity and end-effector velocity. The CN is the maximum ratio of the *relative error* in $\dot{q}$ divided by the *relative error* in $\dot{x}$:

$$\frac{\left\|J^{-1}e\right\|}{\left\|J^{-1}\dot{x}\right\|} \Big/ \frac{\|e\|}{\|\dot{x}\|} \tag{2}$$

https://doi.org/10.1017/S0263574718000759 Published online by Cambridge University Press

where e is the error in $\dot{x}$. Assuming that J is a nonsingular matrix, the error in the solution $J^{-1}\dot{x}$ is $J^{-1}e$. The maximum value is the product of the two operator norms:

$$\begin{aligned}\max_{e,\dot{x}\neq 0}\left(\frac{\left\|J^{-1}e\right\|}{\|e\|}\right)\cdot\left(\frac{\|\dot{x}\|}{\left\|J^{-1}\dot{x}\right\|}\right)&=\left(\max_{e\neq 0}\frac{\left\|J^{-1}e\right\|}{\|e\|}\right)\cdot\left(\max_{\dot{x}\neq 0}\frac{\|\dot{x}\|}{\left\|J^{-1}\dot{x}\right\|}\right)\\&=\left(\max_{e\neq 0}\frac{\left\|J^{-1}e\right\|}{\|e\|}\right)\cdot\left(\max_{\dot{q}\neq 0}\frac{\|J\dot{q}\|}{\|\dot{q}\|}\right)=\left\|J^{-1}\right\|\cdot\|J\|\,.\end{aligned}\tag{3}$$

The CN depends on the choice of norm. If $\|\cdot\|$ is the norm defined in the sequence space ℓ^2, which matches the usual distance in a standard Euclidean space, then

$$\mathrm{CN}=\frac{\sigma_{\max}}{\sigma_{\min}}\tag{4}$$

where $\sigma_{\max}$ and $\sigma_{\min}$ are the largest and smallest singular values of the Jacobian matrix, respectively.[5,13,14] The velocity of the end-effector has isotropy if the calculated value is close to one, and this could be visualized using ME.

3.2. Manipulability ellipsoid (ME)

The ME is an analytical tool for measuring dexterity, like CN, and proposed by Yoshikawa.[6] The manipulability of a manipulator arm can be defined as

$$\eta=\sqrt{\det\left(\boldsymbol{J}\boldsymbol{J}^{\mathrm{T}}\right)},\ (n\geq m)\,,\tag{5}$$

and may be considered as an ellipsoid in the Cartesian space using the following equation:

$$\dot{\boldsymbol{q}}^{\mathrm{T}}\dot{\boldsymbol{q}}=1\tag{6}$$

Combining Eqs. (1) and (6) yields

$$\dot{\boldsymbol{x}}^{\mathrm{T}}\boldsymbol{J}^{-\mathrm{T}}\boldsymbol{J}^{-1}\dot{\boldsymbol{x}}=1\tag{7}$$

where $\boldsymbol{J}^{-1}$ is the inverse matrix. Eq. (7) is called the velocity ME. The principal axes of the ellipsoid are the largest and smallest singular values of the Jacobian matrix of Eq. (7). Therefore, the ratio $(\sigma_{\max}/\sigma_{\min})$ of the principal axes is equal to the CN.

3.3. Modified dynamic conditioning index

Serial-type manipulator arm is generally able to perform rotational motions; hence, one of the important factors in this manipulator design process is to consider the moment of inertia of each linkage of the BDSM arm. In this regard, the previously proposed dynamic conditioning index (DCI) is utilized because quantifying the difference between the generalized inertia matrix derived from the equation of motion and the one from an isotropic matrix is possible using this index.[15] The DCI is defined as follows:

$$\mathrm{DCI}\equiv 0.5d^{\mathrm{T}}Wd\tag{8}$$

where W is a diagonal matrix, and d is a vector consisting of the upper triangular components of matrix D. Matrix D is derived from the difference between the generalized inertia and isotropic matrices

$$D\equiv M-\sigma I\tag{9}$$

where M is a generalized inertia matrix; σ is a positive scalar one; I is an $n\times n$ identity matrix; and d is an $n(n+1)/2$ dimensional vector expressed as follows:

$$d\equiv\left[I_{11}-\sigma\ \cdots\ I_{nn}-\sigma\ I_{12}\ \cdots\ I_{1n}\ I_{23}\ \cdots\ I_{n-1,n}\right]^{\mathrm{T}}\tag{10}$$

https://doi.org/10.1017/S0263574718000759 Published online by Cambridge University Press

As mentioned before, the BDSM arm must perform common motions, such as the vertical and horizontal backward-forward motions in the confined cell. In this regard, minimizing the variation of the generalized inertia matrix of the arm along the considered paths could be a better choice compared to making a generalized inertia matrix for a given configuration close to an isotropic matrix. The MDCI is utilized to quantitatively represent this issue.[16] This MDCI is based on the decoupled form derived by applying the congruence transformation to the generalized inertia matrix[13] and defined as follows:

$$\text{MDCI} \equiv \frac{1}{2} d_N^T d_N \tag{11}$$

where d_N is an n-dimensional vector, and its elements are presented as follows:

$$d_N \equiv \left[\delta N_1 \ \delta N_2 \ \cdots \ \delta N_{n-1} \ \delta N_n\right]^T \tag{12}$$

$$\delta N_k = \max_{t\epsilon(t_0,t_f)} N_k - \min_{t\epsilon(t_0,t_f)} N_k, \quad (k = 1, \cdots, n) \tag{13}$$

where N_k has the decoupled form of the generalized inertia matrix shown in Eq. (14):

$$\begin{bmatrix} N_1 & \cdots & 0 \\ \vdots & \ddots & \vdots \\ 0 & \cdots & N_n \end{bmatrix} \tag{14}$$

4. Design Parameter Optimization Using the Performance Index

This section presents the methodology used to optimize the design parameters with a direct influence on the original performance and its analysis for the BDSM arm. A performance analysis was conducted by discretely separating the kinematic and dynamic attributes of the BDSM. CN and ME were utilized for the kinematic analysis, and MDCI was applied to measure the dynamic performance of the BDSM arm. The optimization of the design parameters was performed as follows: first, the design parameter was reduced by simplifying the linkage shape; second, the initial posture and linkage length were selected by formulating the objective function using a kinematic performance index; and third, the energy efficiency was minimized using the objective function derived from the dynamic performance index.

4.1. Selection of the design parameter

The typical parameters influencing the manipulator arm's performance were linkage length, link mass, and inertia. These three factors were dependent on each other; hence, designing while exclusively considering only one factor was impossible. In this regard, parameter reduction was performed by simplifying the linkages of the target manipulator arm as a cylindrical shape to improve the simulation efficiency (Fig. 7).

4.2. Design optimization

First, CN was applied to improve the dexterity from the kinematic aspect. However, the objective function must be modified to avoid a singular value:

$$\text{Objective function} : 1 - \frac{1}{\text{CN}} \tag{15}$$

Using the modified objective function and the considered variables, convergence was possible while avoiding the singular value. As stated earlier, the target motions for optimization were vertical and horizontal motions while maintaining the same posture of a gripper; therefore, the initial pose of the manipulator arm was determined and optimized by simplifying the 6-DOF structure to a 3-DOF planar structure. When the BDSM arm performs the considered motions, it may be incapable of performing

https://doi.org/10.1017/S0263574718000759 Published online by Cambridge University Press

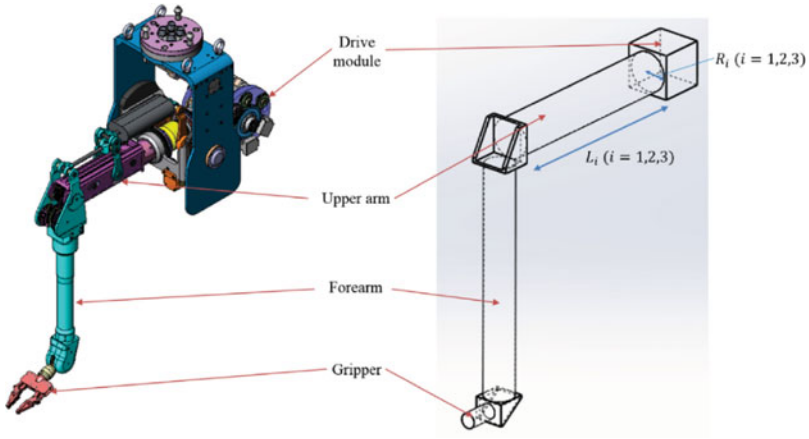

Fig. 7. Defined design parameters of the BDSM arm.

some motions unless the velocity vector components of the end-effector are isotropic. Therefore, the initial pose was considered as a design parameter. Based on this concept, optimization models could be organized as follows to represent problem choices as decision variables and seek for values that minimize the objective functions of the decision variables subject to constraints on variable values, thereby expressing the limits on possible decision choices.

Find
$L_1,\ L_2,\ L_3,\ q_1,\ q_2,\ q_3$

Objective function
$\min\left(1-\frac{1}{\mathrm{CN}}\right)$

Subject to
lower bound $\leq L_i,\ q_i \leq$ upper bound, $(i = 1, 2, 3)$

As a next step, the MDCI was utilized to improve the performance from the dynamic aspect. The kinetic energy of the optimized design was then compared with the original design. Only the diameter of each linkage was changed to maintain the previously optimized kinematic performance. The linkage length remained at the same value with the result of the kinematic optimization. The optimization model for the dynamic performance can be represented as follows:

Find
$R_1,\ R_2,\ R_3$

Objective function
min(MDCI)

Subject to
lower bound $\leq R_i \leq$ upper bound, $(i = 1, 2, 3)$

4.3. Optimization results of the considered design parameters

The design parameters of the BDSM arm were optimized and compared with the original using the approach presented in the previous section. This optimization problem was solved using a GA

https://doi.org/10.1017/S0263574718000759 Published online by Cambridge University Press

Table I. Optimization results of kinematic performance.

Parameters		Initial	Optimal
Link parameters	L_1	0.6 m	0.8 m
	L_2	0.8 m	0.5 m
	L_3	0.3 m	0.2 m
	q_1	0	0.25π
	q_2	-0.5π	-0.8π
	q_3	0.5π	0.55π
Objective function	$1-\frac{1}{\mathrm{CN}}$	0.7539	0.0168

optimization tool included in MATLAB®. The kinematic problem for the optimization of BDSM arm is defined as follows:

Find
$L_1,\ L_2,\ L_3,\ q_1,\ q_2,\ q_3$

Objective function
$\min\left(1-\frac{1}{\mathrm{CN}}\right)$

Subject to
$0.5\,\mathrm{m} \le L_1 \le 0.8\,\mathrm{m},\ 0 \le q_1 \le \mathrm{pi}/4,$
$0.5\,\mathrm{m} \le L_2 \le 0.8\,\mathrm{m},\ -\mathrm{pi}/2 \le q_2 \le -3\mathrm{pi}/4,$
$0.2\,\mathrm{m} \le L_3 \le 0.5\,\mathrm{m}$

The results in Table I were obtained after solving the presented optimization problem. Fig. 8 shows the visualized results using ME. Recall that the manipulator arm provided a better performance as the objective function approached closer to zero. The result showed that the kinematic performance improved by 91.1% after optimization. Fig. 8(a) shows the ME of the initial pose of the original design value. While Fig. 8(b) presents the ME in the joint range associated with the original design. Fig. 8(c) depicts the ME of the initial pose of the optimized design value, while Fig. 8(d) illustrates the ME in the joint range associated with the optimized design. The average value of the optimized objective function was 0.3604 and based upon this result. The performance related with this parameter improved by 35.73% on average.

The optimization problem for the dynamic performance of the BDSM arm is presented as follows:

Find
$R_1,\ R_2,\ R_3$
Objective function
min(MDCI)
Subject to
$0.05\,\mathrm{m} \le R_1 \le 0.08\,\mathrm{m},$
$0.04\,\mathrm{m} \le R_2 \le 0.07\,\mathrm{m},$
$0.03\,\mathrm{m} \le R_3 \le 0.06\,\mathrm{m}$

The worst case for the manipulator arm's motion was considered to acquire a better result for the optimization of dynamic performance, specifically, the case in which every joint was assumed to rotate with a maximum velocity of π rad/s. The results in Table II and Fig. 9 were obtained after solving the designed optimization problem. A comparison of the kinetic energy changes of the original design shown in Fig. 9(a) to that for the optimized design shown in Fig. 9(b) indicated that the performance of the optimized design improved by 16.9% and 39.8%, respectively, compared to the original in terms of the objective function and the maximum value of the kinetic energy. These results showed the improved performance of the modified design in terms of power saving, indicating that the modified design could have a higher performance even if it uses the same level of energy as the original design. This feature could also be applied to operators, who handle the master device

https://doi.org/10.1017/S0263574718000759 Published online by Cambridge University Press

Table II. Optimization results for dynamic performance.

Parameters		Initial	Optimal
Link parameters	R_1	0.08 m	0.054 m
	R_2	0.06 m	0.04 m
	R_3	0.03 m	0.03 m
Objective function	MDCI	1912.1	1589.3

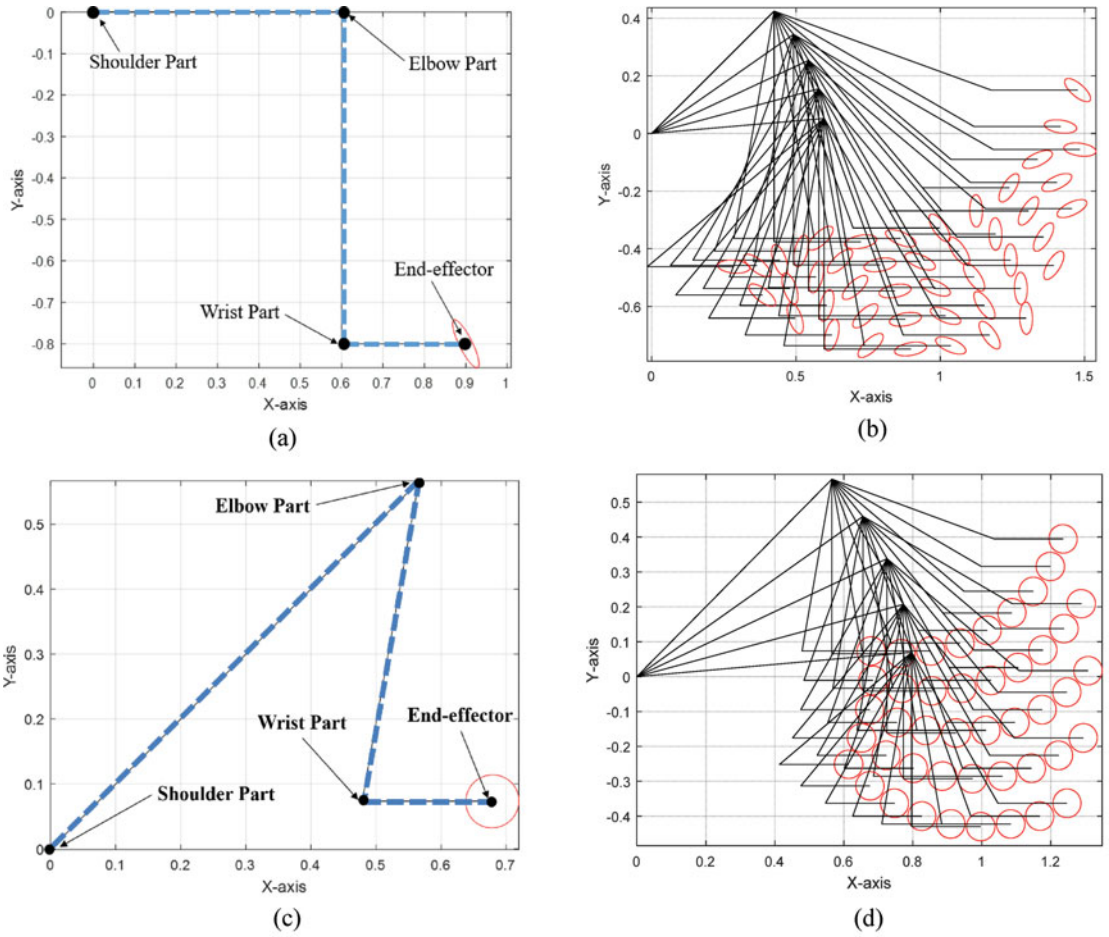

Fig. 8. Manipulability ellipsoid (ME) of the BDSM arm. (a) ME on the initial pose of the original design. (b) ME of the original design in the allowable motion range. (c) ME on the initial pose of the optimized design. (d) ME of the optimized design in the allowable motion range.

with the same configuration as the slave manipulator. Operators generally manipulate the master by grasping the grip equipped at the wrist part of the master device; therefore, if the master has same configuration as the slave, users would feel more comfortable with the modified device than with the original device because the modified device requires less energy to perform the same manipulation task than the original device.

5. Further Study

Apart from the result presented in the previous section, the articulated manipulator arm had an intrinsic feature for the working space. Previously presented Fig. 4 shows that this type of manipulator arm has a different area of unreachable space along the z-axis. This feature might not be a serious problem in industrial applications because the articulated robot generally performs the programmed tasks along the originally defined pathway as an automation system. However, teleoperation tasks generally

https://doi.org/10.1017/S0263574718000759 Published online by Cambridge University Press

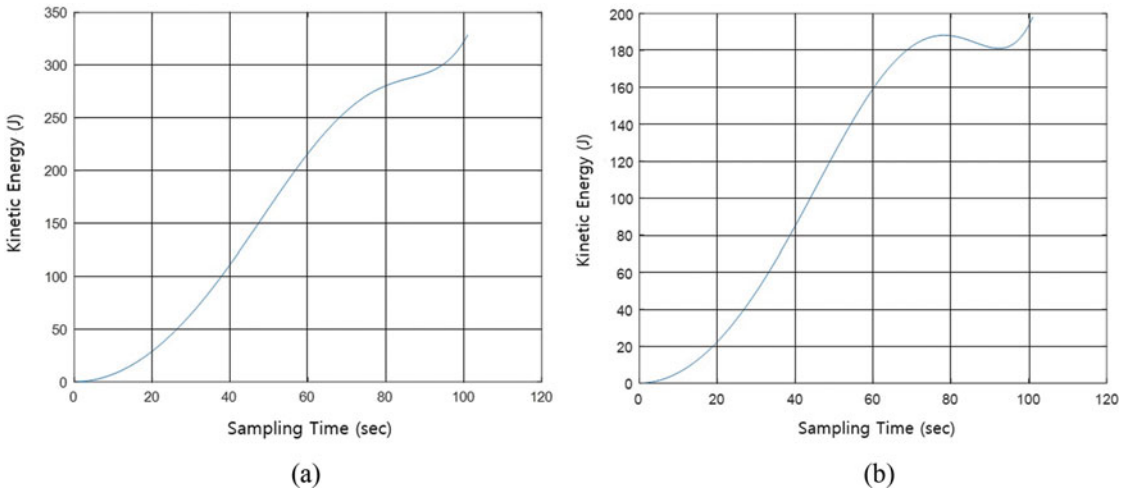

Fig. 9. Kinetic energy of the BSDM. (a) Kinetic energy of the initial design (max. 328.5 J). (b) Kinetic energy of the optimal design (max. 197.9 J).

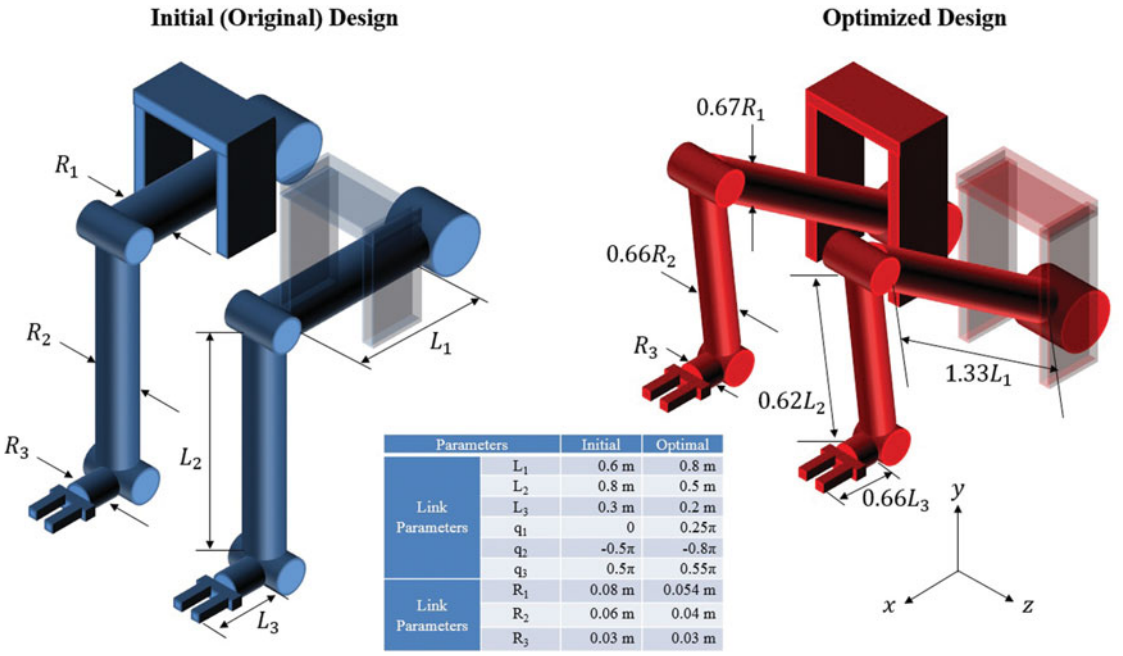

Parameters		Initial	Optimal
Link Parameters	L_1	0.6 m	0.8 m
	L_2	0.8 m	0.5 m
	L_3	0.3 m	0.2 m
	q_1	0	0.25π
	q_2	-0.5π	-0.8π
	q_3	0.5π	0.55π
Link Parameters	R_1	0.08 m	0.054 m
	R_2	0.06 m	0.04 m
	R_3	0.03 m	0.03 m

Fig. 10. Comparison of the original and the modified configuration of the BDSM.

require well-arranged and stable motions to the applied telemanipulator in the entire working envelope because the operator of a teleoperation system only has a limited vision system to recognize the entire pose of the slave system located in the remote area; therefore, minimizing the unexpected dead-zone of the working space during the free motion is important to cover every point of the working space even when the pose of the main body of the slave is not well-arranged against the target object. In this regard, a modified arm configuration of the BDSM could be additionally considered beyond the result of Fig. 10 by rotating the shoulder joint along the x-axis by 90° for the right-side arm and −90° for the left-side arm. The effect of gravity was not considered in the previous optimization process; hence, the change of configuration against the optimized result in Fig. 10 would not harm the originally expected performance. Fig. 11 demonstrates that this manipulator has a SCARA-type arm configuration, and high rigidity could be expected along the vertical direction (y-axis) while maintaining the well-arranged linear motion in the *x*–*z* plane, as proposed in the previous chapter. This performance could be highly effective in the considered teleoperation facility because the working envelope generated by

https://doi.org/10.1017/S0263574718000759 Published online by Cambridge University Press

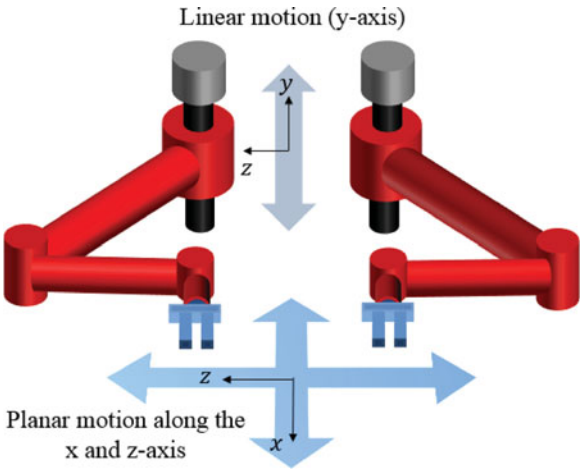

Fig. 11. Configuration of the conceptually modified BDSM (SCARA type).

the modified BDSM of Fig. 11 was appropriate for horizontal motions while maintaining high stability against the vertical loads. Moreover, operators do not need to be concerned about the horizontally correct motion of the slave manipulator arm when they maneuver the backward–forward motion of the slave manipulator arm using the master device. In cases of teleoperation tasks using the articulated-type manipulator, operators find it difficult to precisely recognize their own motion while operating a master device because the master device, including the slave manipulator of the articulated type, could excessively perform free motion in the sagittal plane, and users could easily misunderstand that their own motions are correct, even if they are actually not, until they check their own motion in the third-person point of view. Therefore, properly limiting the DOF of the telemanipulator could be an important issue if the system must perform free and correct motions mostly in a remote area.

6. Conclusions

This study performed a design parameter optimization for a 6-DOF telemanipulator using several kinds of kinematic and dynamic analysis methods. The existing manipulator was designed as a 6-DOF dual-arm structure to cover the various motions performed in the remote area. However, dominant motions were found through long-term field tests, and requirements were devised for design improvements dedicated to the dominant motions while maintaining the DOF of the manipulator. In this regard, CN and ME were applied to investigate the original and optimized design parameters based on the modified initial pose considering enhanced isotropy. The configuration of the considered manipulator arm was modified through this process. The dynamic performance optimization was performed using the modified linkage length derived from the previous optimization process while changing the radius of each linkage. Finally, the MDCI was applied to reduce the kinetic energy for the fully actuated joints. The optimized design performance was also quantitatively verified. Fig. 10 shows the changes made to the configuration through the optimization process performed herein. The modified manipulator arm configuration could be used as a design guideline for future telemanipulator systems in various kinds of hot cell facilities with similar motions to those considered in this study. The proposed design process could also be utilized to design telemanipulator systems that are optimally configured for specified telemanipulation tasks.

Acknowledgments

This work was supported by the Nuclear Research & Development Program of the National Research Foundation of Korea (NRF) funded by the Ministry of Science, ICT and Future Planning (MSIP).

References

1. X. J. Liu, J. Wang and G. Pritschow. “Performance atlases and optimum design of planar 5R symmetrical parallel mechanisms,” *Mech. Mach. Theory* **41**, 119–144 (2006).

2. B. K. Rout and R. K. Mittal, "Screening of factors influencing the performance of manipulator using combined array design of experiment approach," *Robot. Comput.-Integr. Manuf.* **25**, 651–666 (2009).
3. J. R. Singh and J. Rastegar, "Optimal synthesis of robot manipulators based on global kinematic parameters," *Mech. Mach. Theory* **30**(4), 569–580 (1995).
4. S. B. Niku, *Introduction to Robotics: Analysis, Systems, Applications* (Prentice Hall, New Jersey, USA, 2001).
5. G. Strang, *Linear Algebra and its Application* (Academic Press, New York, 1976).
6. T. Yoshikawa, "Manipulability of robotic mechanisms," *Int. J. Robot. Res.* **3**, 3–9 (1985).
7. S. W. Hwang, H. G. Kim, Y. S. Choi, K. S. Shin and C. S. Han, "Design optimization method for 7 DOF robot manipulator using performance indices," *Int. J. Precis. Eng. Manuf.* **18**(3), 293–299 (2017).
8. J. H. Holland, *Adaptation in Natural and Artificial Systems* (University of Michigan Press, Michigan, USA, 1975).
9. I. J. Cho, G. S. You, W. M. Choung, E. P. Lee, D. H. Hong, W. K. Lee, J. H. Ku, S. I. Moon, K. C. Kwon and K. I. Lee, Development of Demonstration Facility Design Technology for Advanced Nuclear Fuel Cycle Process, Technical Report of Korea Atomic Energy Research Institute, No. KAERI/RR-3414/2012 (2012).
10. J. H. Ku, S. I. Moon, I. J. Cho, W. M. Choung, G. S. You and H. D. Kim, "Development of pyroprocess integrated inactive demonstration facility," *Procedia Chem*. **7**, 779–784 (2012).
11. J. K. Lee, H. J. Lee, B. S. Park and K. Kim, "Bridge-transported bilateral master-slave servo manipulator system for remote manipulation in spent nuclear fuel processing plant," *J. Field Robot.* **29**(1), 138–160 (2012).
12. B. S. Park, J. K. Lee, H. J. Lee, S. N. Yu and K. H. Kim, "Remote Modular Design for a Bridge Transported Dual Arm Servo-Manipulator Applied in Pyroprocessing Facility," *Proceedings of the IEEE 11th International Conference on Control, Automation and Systems (ICCAS)* (2011) pp. 1708–1711.
13. J. Angeles and C. S. Lopez-Cajun, "Kinematic isotropy and the conditioning index of serial robotic manipulators," *Int. J. Robot. Res.* **11**(6), 560–571 (1992).
14. J. P. Merlet, "Jacobian, manipulability, condition number, and accuracy of parallel robots," *J. Mech. Des.* **128**(1), 199–206 (2006).
15. O. Ma and J. Angeles, "The Concept of Dynamic Isotropy and its Applications to Inverse Kinematics and Trajectory Planning," *Proceedings of the IEEE International Conference on Robotics and Automation*, vol. **1** (1990) pp. 481–486.
16. T. A. Loduha and B. Ravani, "On first-order decoupling of equations of motion for constrained dynamical systems," *Trans. ASME*, **62**, 216–222 (1995).